Joshua J. Whiting
Richard D. Sacks

Department of Chemistry, University of Michigan, Ann Arbor, MI, USA

Original Paper

Evaluation of split/splitless operation and rapid heating of a multi-bed sorption trap used for gas chromatography analysis of large-volume air samples

The effects of split-flow operation and rapid trap heating on injection-plug widths from an electrically heated, microscale, multibed sorption trap were evaluated. The sorption trap has been designed to quantitatively collect volatile organic compounds from large-volume vapor samples and inject them into a gas chromatograph. Previous trap designs resulted in injection-plug widths of typically a second or more, and this significantly degraded chromatographic resolution, particularly for early-eluting sample components and for high-speed separations. Injection-plug widths are determined by the heating rate of the trap during sample desorption and the volumetric flow rate of carrier gas through the trap. The effects of the heating rate of the trap and carrier gas velocity through the trap on the injection-plug widths of pentane, octane, and undecane were studied. Carrier gas velocity through the trap was increased by splitting the flow coming from the trap between the column and a vent. This decreases transport time from the trap to the column, and thus decreases injection-plug widths. The heating rate for the trap was increased by increasing the applied voltage in the range from 4 to 30 V. Increasing the heating rate decreases the time required to desorb the analytes from the sorbent bed, thus decreasing injection-plug width. Injection-plug widths as small as 89, 210, and 520 ms were obtained in the split mode with very fast heating rates for *n*-pentane, *n*-octane, and *n*-undecane, respectively. The effect of split ratio on resolving power, peak height, and peak width was also evaluated.

Keywords: Heating rate / Injection-plug width / On-line preconcentrator / Split/splitless operation

Received: July 12, 2005; revised: September 2, 2005; accepted: October 17, 2005

DOI 10.1002/jssc.200500276

1 Introduction

The GC analysis of organic compounds in large-volume vapor samples is important in a variety of applications including ambient air analysis, human breath analysis, and both static and dynamic headspace analyses. Analytical methods for these applications usually involve a sorption trap or cryogenic trap for the collection and injection of the organic compounds. For on-site analysis, cryogenic traps are inconvenient since cryogenic materials must be transported to the analysis site. Sorption traps require no cryogenic materials, but often produce injection plugs that are too wide for high-speed GC with capillary columns. This limitation is particularly serious for very volatile compounds, which benefit little from on-column focusing with temperature-programmed GC.

On-site sample collection in canisters or sorption traps followed by transportation of collected samples to a laboratory for analysis is common, but the risk of sample loss or alteration during transportation and storage as well as much longer analysis turnaround times are significant limitations [1]. Biogenic compounds including terpenes and aldehydes are particularly prone to decomposition [2, 3] during storage and thermal desorption from traps [4 – 7].

Recently, microscale sorption traps have been used successfully for the collection of organic compounds from large-volume vapor samples and the injection of the col-

Correspondence: Professor Richard D. Sacks, University of Michigan, 930 N. University Ave., Ann Arbor, MI 48109, USA.
E-mail: rdsacks@umich.edu.
Fax: +1-734-647-4865.

Abbreviations: FID, flame ionization detector; **HV**, high voltage; **LV,** low voltage

lected sample as a vapor plug sufficiently narrow for GC analysis with capillary columns [8–11]. A microscale, multibed trap, which uses a graded series of carbon-based adsorbents, was described by Lu and Zellers [12, 13]. The discreet beds are arranged so that sample gas flow is in the direction from the weakest (lowest surface area) to the strongest bed. The highest boiling point compounds are completely stripped from the sample by the first bed encountered, thus protecting the stronger beds from these compounds, which would be difficult to thermally desorb. Prior to thermal desorption, gas flow direction through the trap is reversed, and carrier gas flow through the device is in the direction from the strongest bed to the weakest bed. This prevents the highest boiling point components in the sample from ever contacting the strongest beds. With this arrangement, quantitative desorption is obtained with no memory effects [10, 11].

Injection-plug characteristics of this multibed trap were studied by Sanchez and Sacks [10, 11]. Thermal desorption was accomplished by the direct resistive heating of the metal trap tube. Injection-plug widths varied from 0.7 to several seconds for compounds in the volatility range from *n*-C5 to *n*-C12. For the higher boiling point compounds, injection-plug widths of greater than 1 s are not a significant problem with temperature-programmed column operation because of efficient on-column focusing on the cold column prior to the initiation of the temperature program [14]. However, for early-eluting compounds, which have substantial migration rates at the column starting temperature, these injection-plug widths severely limit chromatographic resolution. The use of cryogenic cooling of a bare metal trap or the head of the chromatographic column to refocus the desorbed injection plug has been shown to significantly enhance the shape of the injection plug [15–21]. For laboratory-based systems, this can work very well; however, for systems designed to be operated in the field for on-site monitoring the need for cryogenic material adds significant inconvenience as well as a consumable which must be monitored and maintained.

Injection-plug width is determined by the combination of desorption time and vapor-transport time. Preliminary studies using a microfabricated trap have demonstrated that desorption time may be reduced by more aggressive heating using heating rates up to 100°C/s [22, 23]; maximum temperature limits of the sorbent materials, heat transfer through the materials, and increased risk of sample decomposition are important issues.

The vapor-transport time can be reduced by increasing the carrier gas flow rate through the trap tube during desorption. However, the increased column flow results in stretching of the injected vapor plug, thus eliminating the advantage of sweeping the trap volume more quickly. Further study of this is ongoing. Alternatively, the trap volume can be purged of sample vapor more quickly by using a high carrier gas flow rate during desorption and venting some of the gas flow (split-flow operation) prior to the separation column. This is similar to split injection for liquid samples injected by conventional syringe methods, [14] and to preliminary studies using a microfabricated preconcentrator [24, 25].

This report considers both rapid heating of the preconcentrator and split-flow operation for reducing injection-plug widths for a multibed sorption trap. The effects of trap heating rate and carrier gas flow rate through the trap on injection-plug width are evaluated, and the effect of on-column focusing of higher boiling-point compounds is illustrated for temperature-programmed chromatograms.

2 Experimental

2.1 Apparatus

Figure 1 shows a diagram of the multibed trap, the separation column and the associated plumbing. Design features of the multibed trap have been described in detail [10, 11]. The trap was similar to a design reported by Lu and Zellers [12, 13]. The trap consisted of four discreet beds labeled C, X, B, and Y. Beds Y, B, and X used three different grades of graphitized carbon, Carbopack Y, Carbopack B, and Carbopack X, respectively. Bed C used carbon molecular sieves, Carboxen 1000. All materials were obtained from Supelco (Bellefonte, PA). Each bed contained about 2 mg of sorbent. This quantity was sufficient to quantitatively trap all target compounds at the concentrations used in this study. The beds are ordered weakest to strongest from right to left in Fig. 1. The beds were separated with glass wool (20834, Supelco) plugs. Stainless steel mesh (Supelco) was used to hold the beds

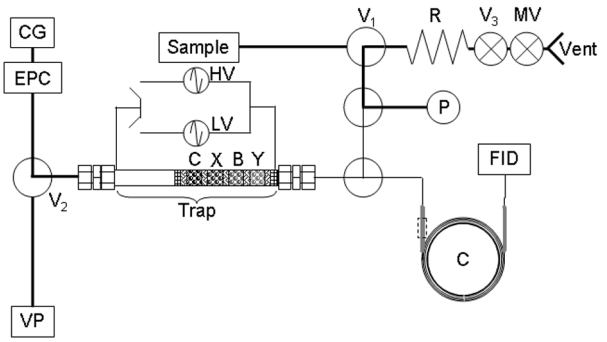

Figure 1. Multibed sorption trap with at-column heated separation column C and associated plumbing for split/splitless operation. Sample gas at atmospheric pressure is pulled through the four adsorption beds from right to left. After sample collection, valves V_1 and V_2 are switched and carrier gas from CG flows through the trap from left to right. See text for details.

in position in an 80-mm long, 1.35-mm ID Inconel 600 tube, a Ni-Co alloy (Accu-Tube, Englewood, CO).

Large-volume vapor samples at atmospheric pressure were introduced into the trap by means of vacuum pump VP (HYVAC-7, Cenco Instruments, Chicago, IL) from right to left through three-way solenoid valves V1 and V2 (01380-05, Cole Parmer, Vernon Hills, IL). Note that the flow direction was from the weakest bed (Y) to the strongest bed (C) during sample collection. After sample collection was complete, V1 and V2 were switched, and carrier gas proceeded from left to right through the trap tube and the separation column C. For splitless operation, two-way solenoid valve V3 (55P18DIA, Valcor, Springfield, NJ) was closed, and all carrier gas flow through the trap also passed through the column. For split-flow operation, V3 was opened, and the split flow was controlled by pneumatic restrictor R, which consisted of an 80-cm long segment of 0.25-mm ID PEEK tubing (Valco Instruments, Houston, TX). The pneumatic restriction was about 1/10 of the column restriction, and thus, when the split valve (V3) was open, the split ratio (split-flow/column flow) was nominally 9 : 1. For most studies, metering valve MV (55-4 μBG, Nupro, Willoughby, OH) was completely open and had no effect on the split ratio. For studies of the effects of split ratio on resolving power, peak width, and peak height, this valve was used to adjust the split ratio. All plumbing lines shown in bold in Fig. 1 were fused-silica lined 1/16-in. OD, 0.04-in ID stainless steel tubing (Restek, Bellefonte, PA). All connecting lines in the sample flow path were of capillary dimension and were heated to eliminate cold spots.

The trap was resistively heated in two stages by ac power provided by Variac autotransformers high voltage (HV) and low voltage (LV). Initial heating at rates as high as 650°C/s was provided by higher spike voltages in the range 4–30 V (HV). In all cases, the pulse duration was set to give a peak trap temperature of 325°C. The pulse duration was controlled by solid-state relays operated from a PC not shown in Fig. 1. The second heating stage lower maintenance voltage (2–4 V) (LV) was used to maintain the trap tube temperature at 325°C for as long as necessary to completely purge the trap of the trapped analytes. This second heating stage was only needed for compounds with boiling points greater than that of *n*-C8.

The separation column was an 8.0-m length of 0.25-mm ID fused-silica coated with a 0.25-μm thick film of nonpolar dimethyl polysiloxane (Rtx-1, Restek). The column was prepared by RVM Scientific, Santa Barbara, CA, for use with high-speed at-column heating. The process consisted of wrapping a colinear ensemble of the fused-silica column, an insulated heating wire, and a sensor wire with fiber insulation. The ensemble was wound into a coil about 7 cm in diameter, and the coil was wrapped with metal foil. These columns can be heated reproducibly at linear rates in excess of 1000°C/min.

For measurements of injection-plug width, the column was replaced with a 21-cm long segment of 0.1-mm ID deactivated fused-silica tubing. This tube provided about the same pneumatic restriction and thus the same volumetric flow rate as the column for a given head pressure. An electronic pressure controller EPC (640A, MKS Instruments, Meuthuen, MA) was used to control the column (or restrictor tube) head pressure, which was measured by gauge P (PX303-050A5V, Omega Engineering, Stamford, CT). A flame ionization detector (FID in Fig. 1) (Varian, Palo Alto, CA) was used for detection. Volumetric flow rate at the detector was measured with a soap-bubble flow meter. Flow rate measurements at the end of the column and at the splitter outlet gave a split ratio of 8.2 : 1. The FID current was monitored with an electrometer built in house and having a time constant of less than 10 ms. The system was interfaced to a PC by means of a 16-bit A/D board (PCI-DAS 1602, Computer Boards, Mansfield, MA).

2.2 Materials and procedures: Test mixture preparation and sampling

Test mixtures were made from the compounds listed in Table 1. All compounds were at least reagent grade.

Table 1. Compounds and boiling points for test mixtures

Label	Compound	BP, °C	Label	Compound	BP, °C
1	Methanol	64.7	21	2-Methyl-heptane	117.6
2	Ethanol	78.4	22	Hexanal	131
3	Acetone	56.5	23	Tetrachloro-ethylene	120.8
4	2-Propanol	82.5	24	Octane	125.6
5	Pentane	36.1	25	Butyl acetate	121
6	Butanal	76	26	Chlorobenzene	132.2
7	2-Butanol	98	27	Ethyl benzene	136.2
8	Hexane	68.7	28	*m*-Xylene	139.1
9	Ethyl acetate	77.1	29	Cyclohexanone	155.6
10	1,2-Dichloro-ethane	57.4	30	Styrene	145.2
11	1,1,1-Trichlor-oethane	74.1	31	Nonane	150.8
12	Benzene	80.1	32	Cumene	152.4
13	1-Butanol	117.5	33	α-Pinene	155
14	2-Pentanone	103.3	34	Mesitylene	164.7
15	Pentanal	103	35	β-Pinene	158.3
16	Trichloro-ethylene	86.7	36	3-Octanol	178.5
17	2,5-Dimethyl-furan	93	37	1,2,3-Trimethyl-benzene	175
18	Heptane	98.4	38	Butyl benzene	183
19	2,5-Dimethyl-hexane	108	39	Nonanal	185
20	Toluene	110.6	40	Undecane	195.8

Vapor samples for single compound and isothermal mixtures were prepared by injecting 1 μL of individual compounds into 1-L Tedlar gas sampling bags (model 232-01, SKC, Eighty Four, PA), diluting with dry filtered air (air which has been filtered to remove water and organic vapors) and allowing to equilibrate at room temperature for ~30 min before use. These bags were sampled for 0.2 – 1 s at a flow rate of ~30 cm^3/min. The vapor sample for the temperature programming study was prepared in a 12-L Tedlar bag (model 232-10, SKC) by injecting 1 μL of low-boiling point compounds and 3 – 5 μL of higher-boiling point compounds. The sample was diluted with dry filtered air, and allowed to equilibrate for ~30 min before use. This bag was sampled for 3 – 10 s. These relatively high concentrations and short sampling times were chosen to expedite testing of the performance of split-flow operation. Performance of this trap design has been described elsewhere for a large-volume air sample with concentration in the ppt to ppm range [8 – 13, 26].

2.3 Materials and procedures: GC operating conditions

Hydrogen carrier gas was purified by filters for hydrocarbons, water vapor, and oxygen. Column starting temperature was 30°C for all runs. For the temperature programming study, delays (isothermal) of 30, 60, and 120 s and programming ramps of 100, 50, and 25°C/min were used for column flow rates of 2, 1, and 0.5 cm^3/min, respectively.

3 Results and discussion

3.1 Injection-plug properties

For these studies, the separation column was removed and replaced with a segment of fused-silica tubing that provided a transport time to the FID of less than 1 s. Under these conditions, band broadening in the tubing was negligible, and the true injection-plug width and shape could be ascertained. Vapor-transport time during desorption was determined by the volumetric flow rate of carrier gas during desorption and the dead volume of the trap tube downstream from the sorption beds as well as the interstitial volume of the sorbent beds. The location and distribution of the trapped analytes in the multibed structure was largely unknown and was probably different for every trapped species. Dead volume was estimated in the range 10 – 20 μL.

Figure 2 shows injection plugs for *n*-pentane obtained with heating rates of 50°C/s (a), 100°C/s (b), and 200°C/s (c) and volumetric flow rates through the trap tube of 0.5 (A), 2.0 (B), 9.3 (C), and 20.8 cm^3/min (D). The two lower flow rates were obtained with splitless operation, and the higher two flow rates were obtained with split operation (split valve open) and flows at the FID of 0.5 and 2.0 cm^3/min, respectively. In all cases, the peak trap temperature was about 325°C, and the LV power supply used to sustain the trap temperature was not used. For each case, about 0.3 μg of pentane was collected in the trap. Peak heights were different for all the cases shown in Fig. 2, but they were adjusted for presentation clarity so that peak widths could be more easily compared.

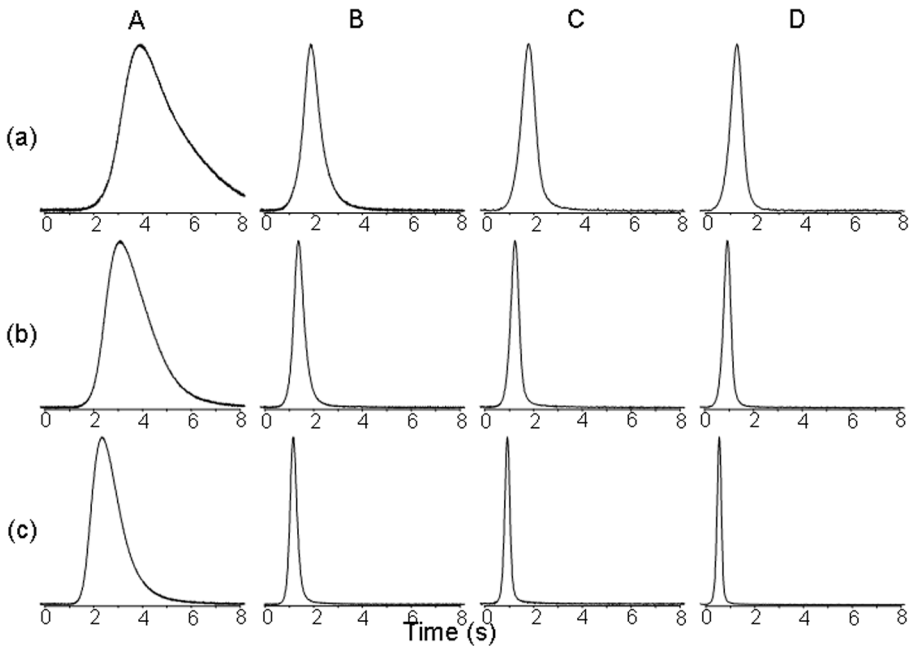

Figure 2. Injection-plug profiles for *n*-C5 with trap heating rates of 50 (a), 100 (b), and 200°C/s (c) with flow rates through the trap tube of 0.5 (column A), 2.0 (B), 9.3 (C), and 20.8 cm^3/min (D). The two higher flow-rate values were obtained with split operation. In all cases, the trap was heated to 325°C.

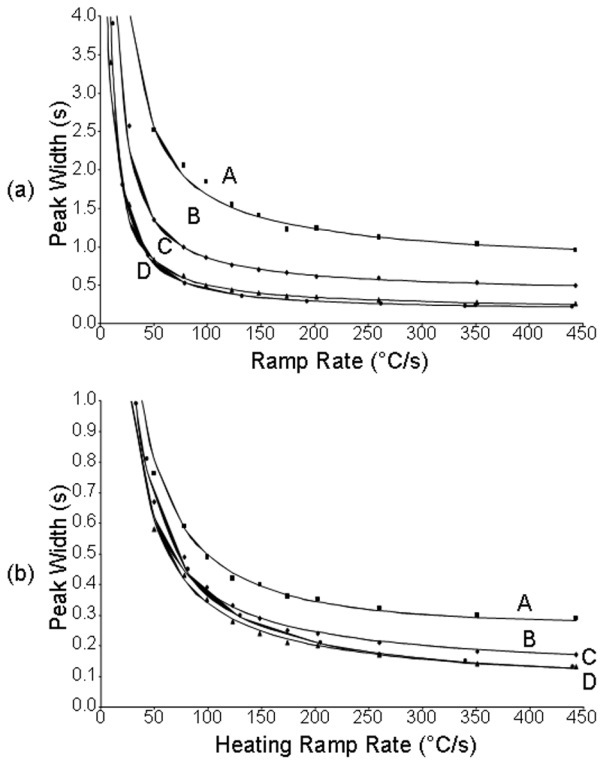

Figure 3. Plots of peak width (full width at half height) *versus* trap heating-ramp rate for *n*-C5 with splitless operation (a) and split operation (b). Carrier gas flow rates at the detector were 0.5 (plots A), 1.0 (B), 2.0 (C), and 3.0 cm^3/min (D). In all cases, the trap was heated to 325°C.

The width of the injection plug decreased steadily with increasing heating rate and with increasing flow rate through the trap. For a carrier gas flow rate through the trap of 0.5 cm^3/min (column A in Fig. 2), which is typical of column flow rates anticipated with microfabricated GC instruments [27, 28], broad injection plugs were observed even with a heating rate of 200°C/s (c). For the highest flow rate of 20.8 cm^3/min, less than 50 ms was required to purge the trap of sample vapor. The injection-plug width (full width at half height) for pentane at this flow rate and using a heating rate of 50°C/s was 0.9 s. This indicates that the injection-plug width was heating-rate limited at this high flow rate. When the heating rate was increased to 200°C/s at a flow rate of 20.8 cm^3/min, the injection-plug width was reduced to about 0.2 s. This is narrower than any previously reported injection plug from a multibed sorption trap.

Figure 3 shows plots of injection-plug width (full width at half height) for splitless operation (a) and split operation (b) *versus* the trap heating ramp rate. For both sets of plots, the inlet pressure was adjusted to give flow rates at the FID of 0.5 (A), 1.0 (B), 2.0 (C), and 3.0 cm^3/min (D) and heating rates ranging from 10 to 450°C/s. In all cases, the peak trap temperature was about 325°C, and the LV power supply used to sustain the trap temperature was not used. Note that the peak width scale has been adjusted for presentation purposes to cover the range from 0 to 4.0 s for splitless operation and 0 to 1.0 s for split operation. In all cases, the peak widths decreased rapidly with increasing heating rate for low heating rate values and became nearly independent of heating rate for the higher heating rates. This suggests that at the lower heating rates, peak width was controlled more by the heating rate, and at the higher heating rates, peak width was controlled more by vapor transport through the trap tube.

For splitless operation, the lowest flow rate of 0.5 cm^3/min through the trap tube (plot A) gave a minimum peak width of about 1 s for a heating rate of 450°C/s. For a flow rate of 2.0 cm^3/min, which is typical for capillary-column GC, the injection-plug width is about 0.24 s. With a heating rate of 650°C/s, which is the highest value used in this study and is not shown in Fig. 3, the injection-plug width was reduced slightly to about 0.21 s. With split operation, the total flow rates through the trap were 4.1, 9.3, 20.8, and 34.8 cm^3/min for plots A, B, C, and D, respectively. For these higher flow rates, all injection-plug widths were less than 1 s even for heating rates as low as 50°C/s. For a heating rate of 450°C/s and flow rates of 20.8 and 34.8 cm^3/min, the injection-plug width was about 0.1 s. At the highest flow rate, a heating rate of 650°C/s gave a pentane peak width of 0.089 s. These values are comparable to injection-plug widths from split injections of liquid samples using commercial instruments.

Figure 4 shows data similar to that shown in Fig. 2 but for *n*-octane. Note the time scale in Fig. 4 extends to 16 s compared to 8 s for Fig. 2. Typically, the injection-plug widths for *n*-octane were about twice those from *n*-pentane for comparable heating rates and flow rates. For the lowest flow rate of 0.5 cm^3/min, broad and severely tailed peaks were observed for all three heating rates. For a heating rate of 200°C/s, the injection-plug tailing for octane was significantly more severe than for pentane. When the flow rate was increased to 2.0 cm^3/min, a heating rate of 200°C/s gave a much more symmetric injection plug with a width of about 1.3 s. At the highest flow rate with the split valve open and a heating rate of 200°C/s, the octane plug width was 0.35 s.

Figure 5 shows plots of peak width *versus* heating rate for *n*-octane with splitless (a) and split (b) operation with flow rates at the FID of 0.5, 1.0, 2.0, and 3.0 cm^3/min for plots A, B, C, and D, respectively. Again heating rates ranged from 10 to 450°C/s, and the peak-width scales for the split and splitless cases were adjusted for presentation clarity using a scale of 0–7 s for splitless and 0–1 s

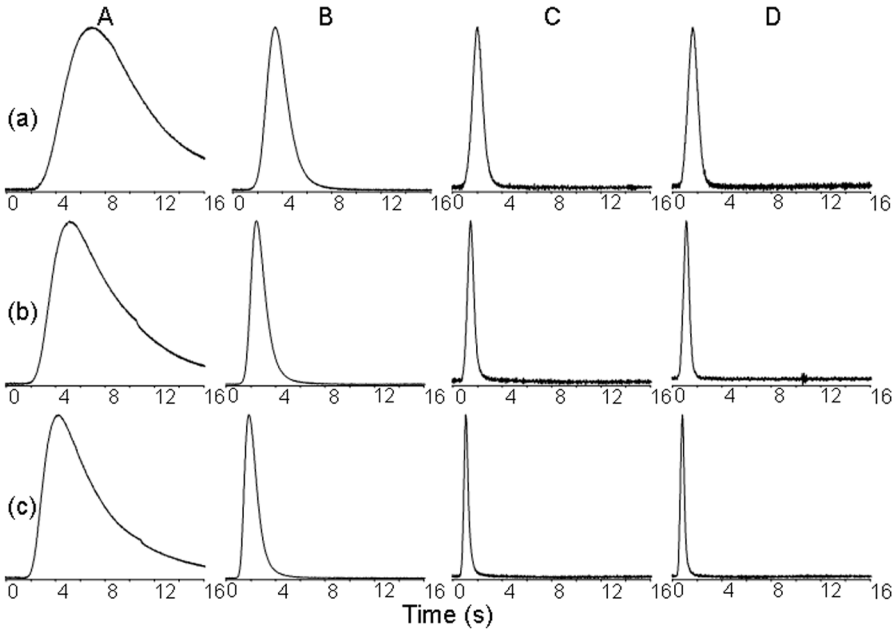

Figure 4. Injection-plug profiles for *n*-C8 with trap heating rates of 50 (a), 100 (b), and 200°C/s (c) with flow rates through the trap tube of 0.5 (column A), 2.0 (B), 9.3 (C), and 20.8 cm³/min (D). The two higher flow-rate values were obtained with split operation. In all cases, the trap was heated to 325°C.

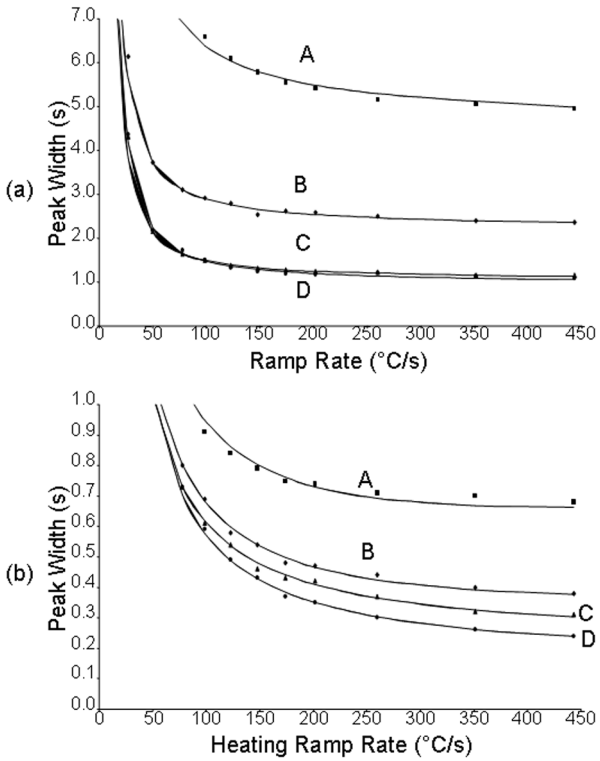

Figure 5. Plots of peak width (full width at half height) *versus* trap heating-ramp rate for *n*-C8 with splitless operation (a) and split operation (b). Carrier gas flow rates at the detector were 0.5 (plots A), 1.0 (B), 2.0 (C), and 3.0 cm³/min (D). In all cases, the trap was heated to 325°C.

for split operation. These data are similar to those for *n*-pentane shown in Fig. 3 but the peak widths are greater for *n*-octane. With splitless injection and a detector flow of 0.5 cm³/min (plot A), the *n*-octane injection-plug width was greater than 5 s for the entire range of heating rates shown in Fig. 5. With split injection, the peak width was reduced to about 0.7 s for the higher heating rates. For detector flow rates of 2.0 and 3.0 cm³/min (plots C and D), splitless injection gave injection-plug widths of about 1 s for the higher heating rates. With split injection, the *n*-octane peak width was reduced to about 0.25 s for a detector flow of 3 cm³/min. For a heating rate of 650°C/s (not shown in Fig. 5), split injection with a detector flow of 3 cm³/min resulted in an injection-plug width of 0.21 s.

For *n*-undecane, the injection-plug width for splitless operation with a 0.5-cm³/min detector flow and a 50°C/s heating rate was over 15 s. With split operation and a heating rate of 200°C/s, the injection-plug width was reduced to about 1.8 s. For split operation with a column flow of 3.0 cm³/min and a heating rate of 450°C/s, the injection-plug width was about 0.5 s. The use of faster heating rates shown here confirms the results of earlier reports [22, 23] on the use of faster heating rates to improve injection-plug width. However, the significantly faster rates used here are necessary to take full advantage of the use of faster trap flow with split operation.

3.2 Isothermal chromatograms

Chromatograms were obtained at 30°C with a 10-m long, nonpolar column. The test mixture in the gas sampling bag contained the first 18 compounds listed in Table 1. Figure 6 shows chromatograms for splitless [(a), (c), and (e)] and split [(b), (d), and (f)] operation with column flow

Table 2. Peak widths and plate number for pentane, heptane, and octane at 30°C for split and splitless operation at different flow rates

Splitless				Split			
0.5 cm³/min	t_R, s	$W_{1/2}$, s	N	0.5 cm³/min	t_R, s	$W_{1/2}$, s	N
Pentane	62.5	1.31	12 600	Pentane	63.1	0.98	23 000
Heptane	136.6	2.22	21 000	Heptane	136.2	1.95	27 100
Octane	279.8	3.97	27 500	Octane	277.3	3.91	27 800
1 cm³/min	t_R, s	$W_{1/2}$, s	N	1 cm³/min	t_R, s	$W_{1/2,}$	N
Pentane	30.3	0.60	14 000	Pentane	30.5	0.42	29 000
Heptane	68.2	0.97	27 000	Heptane	69.4	0.83	39 000
Octane	140.5	1.80	33 800	Octane	140.9	1.68	39 000
2 cm³/min	t_R, s	$W_{1/2}$, s	N	2 cm³/min	t_R, s	$W_{1/2}$, s	N
Pentane	14.7	0.31	12 000	Pentane	14.8	0.24	21 000
Heptane	33.2	0.53	22 000	Heptane	34.2	0.47	29 000
Octane	68.6	1.04	24 100	Octane	70.5	0.94	31 000

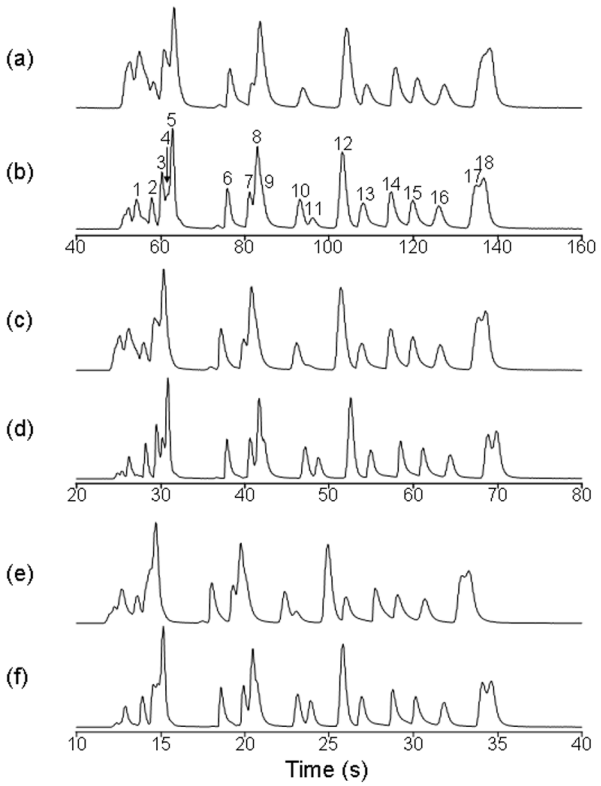

Figure 6. Isothermal chromatograms at 30°C of a mixture containing the first 18 compounds in Table 1 with splitless operation [(a), (c), and (e)] and split operation [(b), (d), and (f)] and column flow rates of 0.5 [(a) and (b)], 1.0 [(c) and (d)], and 2.0 cm³/min [(e) and (f)].

rates of 0.5 [(a) and (b)], 1.0 [(c) and (d)], and 2.0 cm³/min [(e) and (f)]. The trap heating rate was 450°C/s.

For all the column flow rates, split operation resulted in substantially narrower peaks, particularly for the early-eluting components. The improvement with split operation was most obvious with the 1.0 and 2.0 cm³/min column flows, since these values were nearer to the optimal carrier gas flow (1.2 cm³/min) for this column with hydrogen carrier gas. Even for components 17 and 18 at the end of the chromatogram, the resolution was significantly greater with split operation for all three column flows.

As expected, the analysis time is reduced by a factor of 4 at a flow rate of 2.0 cm³/min relative to 0.5 cm³/min, and at the higher flow rate, all 18 components elute in less than 35 s. In Table 2, split and splitless operations are compared with respect to peak widths, and number of theoretical plates for *n*-pentane, *n*-heptane, and *n*-octane for three different column flows. Measurements were made from chromatograms of simple mixtures where the *n*-alkane peaks were completely resolved. Chromatograms were obtained isothermally at 30°C. Plate number N was calculated from the equation $N = 5.45\ (t_R/W_{1/2})^2$, where t_R is the peak retention time and $W_{1/2}$ is the full width at half maximum height.

Since *n*-pentane (peak 5) is an early-eluting compound, which undergoes less on-column band broadening, the peak width and plate number were most improved by the use of the inlet splitter, and for a flow rate of 1.0 cm³/min, the plate number was more than doubled relative to the case without the inlet splitter. For *n*-octane with a column flow of 0.5 cm³/min, the peak width is only slightly smaller with split operation, but at the two higher flow rates, substantial reductions in peak width and increases in plate number were obtained.

An important feature of the chromatograms in Fig. 6 was that the peak area for component 11 (1,1,1-trichloroethane) relative to the other peak areas was substantially

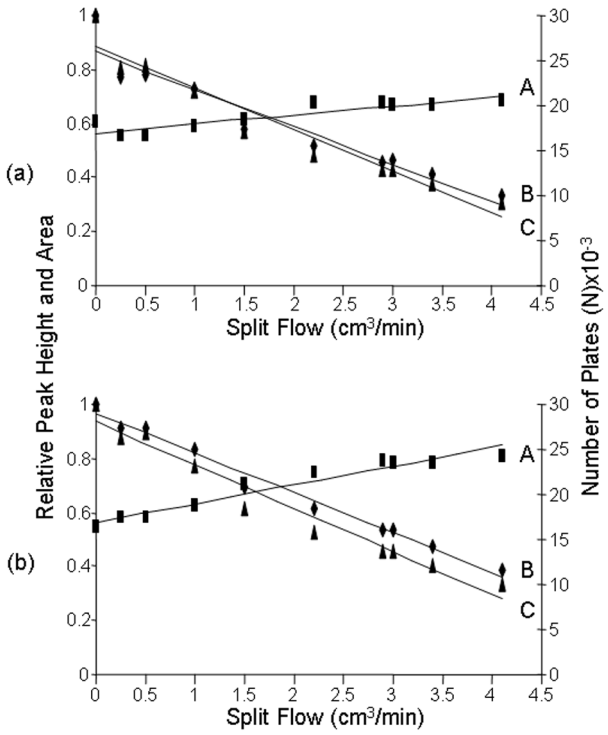

Figure 7. Plots of plate number (A), relative peak heights (B), and relative peak areas (C) *versus* split flow for a column flow of 0.5 cm^3/min. Plots (a) are for *n*-C5, and plots (b) are for *n*-C8.

smaller with splitless operation for all three column flow rates. For a column flow rate of 0.5 cm^3/min, peak 11 was completely absent with splitless operation. As the column flow was increased, the relative peak area for peak 11 increased for both split and splitless operations. Also note that one or more peaks were observed to elute before peak 1, and this peak(s) was more dominant with splitless operation and with reduced column flow.

These data suggest that the very polar 1,1,1-trichloroethane partially decomposed during thermal desorption from the trap, and that this decomposition was reduced by reducing the contact time of the desorbed vapor with the heated adsorbant. Both chloromethane and dichloromethane have retention times consistent with the early-eluting contaminant peak(s) observed in Fig. 6, and are suggested as possible decomposition products. Thus, split operation is useful not only in greatly reducing injection-plug widths but also in reducing thermal degradation of labile compounds. This improved recovery of the target compound and reduced the risk of decomposition products interfering with other target compounds.

The most significant limitation of split operation is the loss in powers of detection due to reduced peak heights and areas for a given sample volume. This is shown in Fig. 7 for *n*-pentane (a) and *n*-octane (b). The trap heating rate was 450°C/s. These plots show the change in plate number (A), peak height (B), and peak area (C) with split flow for the case of a 0.5-cm^3/min column flow. Peak heights and areas are normalized to give values of 1.0 for splitless operation (zero split flow). For both compounds, the peak heights and areas decreased steadily with increasing split flow, and with a split flow of 4.1 cm^3/min (a split ratio of 8.2 : 1), both peak heights and areas are reduced to 30 – 40% of the splitless values. It is important to note that these plots show the expected linear trends as opposed to the nonlinear trends shown in the earlier study by Lu and Zellers [25]. This is probably due to maintaining a constant column flow throughout the present study.

3.3 Temperature-programmed chromatograms

Figure 8 shows temperature-programmed chromatograms for splitless [(a), (c), and (e)] and split [(b), (d), and (f)] operation with column flow rates of 0.5 [(a) and (b)], 1.0

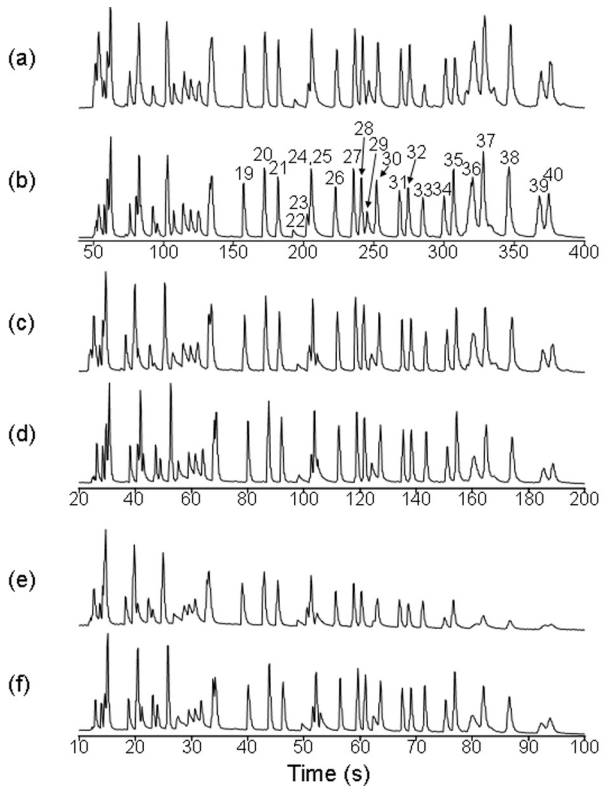

Figure 8. Temperature-programmed chromatograms of the 40-component mixture in Table 1 with splitless [(a), (c), and (e)] and split [(b), (d), and (f)] injection and column flow rates of 0.5 [(a) and (b)], 1.0 [(c) and (d)], and 2.0 cm^3/min [(e) and (f)]. For (a) and (b), a 30°C isothermal interval of 120 s was followed with a programming rate of 25°C/min. For (c) and (d), a 30°C isothermal interval of 60 s was followed with a programming rate of 50°C/min. For (e) and (f), a 30°C isothermal interval of 30 s was followed with a programming rate of 100°C/min.

Table 3. Injection-plug widths compared to temperature-programmed peak widths from Fig. 8 for *n*-undecane using split and splitless operation

Column flow fate, cm^3/min	Splitless injection-plug width	Split injection-plug width	Splitless temperature programming peak width	Split temperature programming peak width
0.5	12.6 s	1.8 s	3.0 s	3.1 s
1	5.0 s	1.0 s	1.6 s	1.5 s
2	2.7 s	0.7 s	– [a]	1.4 s

[a] Peaks were not resolved enough to get an accurate peak width measurement.

[(c) and (d)], and 2.0 cm^3/min [(e) and (f)]. The test mixture in the gas sampling bag contained all 40 compounds listed in Table 1. The trap heating rate was 450°C/s, and the lower voltage power supply was used to maintain the trap temperature at 325°C for 45 s. Temperature programming rates were 25°C/min for chromatograms (a) and (b), 50°C/min for (c) and (d), and 100°C/min for (e) and (f). These values were chosen to give a temperature change of about 20°C during an interval equal to the column holdup time. Previous studies have shown that larger temperature changes result in substantial losses in resolution [29, 30]. To prevent loss of resolution for the early-eluting components, isothermal operation at 30°C was used for 120 s for (a) and (b), 60 s for (c) and (d), and 30 s for (e) and (f). These values of isothermal interval resulted in the temperature program beginning at about the same point (elution time of component 16) for all chromatograms.

For the later eluting compounds, significant on-column focusing occurs, and this reduced problems associated with the wide injection plugs for these compounds with splitless injection [14]. For these later eluting compounds, peak widths decreased steadily with increasing column flow and increasing temperature programming rate, but were nearly identical for split and splitless operations. This is illustrated in Table 3 for *n*-C11 for three different column flows. With splitless injection, injection-plug widths for *n*-C11 with a column and trap flow of 0.5 cm^3/min was over 12 s while the elution peak width was only 3.1 s. With this column flow and split injection, the peak width was not significantly different than the case with splitless injection despite the fact that the injection-plug width was reduced from 12.6 to 1.8 s. Thus, for *n*-C11, the peak width was not significantly affected by the injection-plug width for widths at least up to 12 s.

At the higher column flow rates, both injection-plug widths and peak widths were reduced, but again, there were no significant differences in the *n*-C11 peak widths between split and splitless injection. Note that for all column flows, peak widths were less than the splitless injection-plug widths. For the highest column flow rate (2.0 cm^3/min), which is also the case with the highest temperature-programming rate, peak widths were only slightly smaller than for the 1-cm^3/min flow rate, but retention times and thus peak separation were reduced by about a factor of 2. The result is substantially poorer resolution, and a reliable peak width could not be obtained for *n*-C11 with splitless injection.

4 Concluding remarks

A principal limitation of the in-line, multibed sorption trap is the relatively broad injection plugs relative to liquid injections using an inlet splitter. Broad injection plugs are the result of the substantial trap dead volume and the finite time required for heating the trap to desorb the analytes. Increasing the column flow rate, which increases the carrier gas flow rate through the trap, can reduce dead time from the inlet dead volume. However, increased band stretching on the column at the higher carrier gas velocity obviates the improvement from reduced trap-volume sweep time. In addition, the higher carrier gas velocity may degrade column performance. However, if the extra carrier gas is vented (split), narrower injection plugs can be obtained without changing the column efficiency.

With sufficiently high carrier gas flow rate through the trap, injection-plug widths are limited by desorption times, which are analyte specific. Injection-plug widths decrease continuously with increasing trap-heating rate. At lower heating rates (less than about 100°C/s for splitless injection), the decrease in injection-plug widths with increasing heating rate is very dramatic. With splitless injection, injection-plug widths become relatively independent of trap heating rate for rates greater than 200°C. With split injection, the trap dead volume contributes less extra-column band broadening, and trap heating rate becomes the limiting factor in determining injection-plug width, and significant reductions in plug width are observed with increasing heating rate at least up to 450°C/s.

The increased volumetric flow rate through the trap with split injection can dramatically reduce injection-plug widths as well as provide milder desorption conditions due to decreased contact time of the desorbed vapor with the hot beds and more rapid transport of the vapor from the hot metal tube. Other tests are needed here with other thermally labile analytes to evaluate this further. With the split ratio used in this study, peak heights and areas are reduced to 30–40% of their splitless values. While this is a significant disadvantage of split inlet operation, increased sample collection time can offset this limitation but may require increased trap size (bed mass) to maintain the same detectibility.

Further studies of the effect of greater bed mass on injection-plug width are needed to evaluate the tradeoffs involved.

The multibed trap system is designed to collect quantitatively organic vapors in the *n*-C5 to *n*-C12 volatility range. Column temperature programming is desirable to cover this range. The higher boiling point compounds can be effectively trapped and refocused at the upstream end of the column if the starting temperature is sufficiently low. For these compounds, the reduction in injection-plug width obtained with split operation may not result in significantly improved resolution.

The authors express their appreciation to the following individuals: Dr. Edward T. Zellers, Dr. Chia-Jung Lu, and Dr. Juan M. Sanchez. Funding for this work was provided by Grant No. R01-OH03692 from the National Institute for Occupational Safety and Health of the Centers for Disease Control and Prevention (NIOSH-CDCP). Additional support provided by the University of Michigan Center for Wireless Integrated Microsystems (WIMS) through the Engineering Research Centers Program of the National Science Foundation under Award No. EEC-9986866 is also gratefully acknowledged.

5 References

[1] Batterman, S. A., Zhang, G. Z., Baumann, M., *Atmos. Environ.* 1998, *32*, 1647 – 1655.

[2] Calogirou, A., Larsen, B. R., Brussol, C., Duane, M., Kotzias, D., *Anal. Chem.* 1996, *68*, 1499 – 1506.

[3] Schrader, W., Geiger, J., Klockow, D., Korte, E. H., *Environ. Sci. Technol.* 2001, *35*, 2717 – 2720.

[4] Hollender, J., Sandner, F., Moller, M., Dott, W., *J. Chromatogr. A* 2002, *962*, 175 – 181.

[5] Cao, X. L., Hewitt, C. N., *J. Chromatogr. A* 1994, *688*, 368 – 374.

[6] Helmig, D., *J. Chromatogr. A* 1996, *732*, 414 – 417.

[7] Dettmer, K., Knobloch, T., Engewald, W., *Fresenius. J. Anal. Chem.* 2000, *366*, 70 – 78.

[8] Lu, C. J., Whiting, J., Sacks, R. D., Zellers, E. T., *Anal. Chem.* 2003, *75*, 1400 – 1409.

[9] Sanchez, J. M., Sacks, R. D., *Anal. Chem.* 2003, *75*, 2231 – 2236.

[10] Sanchez, J. M., Sacks, R. D., *Anal. Chem.* 2003, *75*, 978 – 985.

[11] Sanchez, J. M., Sacks, R. D., *J. Sep. Sci.* 2005, *28*, 22 – 30.

[12] Lu, C. J., Zellers, E. T., *Anal. Chem.* 2001, *73*, 3449 – 3457.

[13] Lu, C. J., Zellers, E. T., *Analyst* 2002, *127*, 1061 – 1068.

[14] Grob, R., *Modern Practice of Gas Chromatography* (3rd edn.), John Wiley and Sons, New York 1995.

[15] Willis, D., *J. Gas Chromatogr.* 1967, *5*, 536 – 538.

[16] Willis, D. E., *Anal. Chem.* 1968, *40*, 1597 – 1600.

[17] Jacques, C. A., Morgan, S. L., *J. Chromatogr. Sci.* 1980, *18*, 679 – 683.

[18] Graydon, J. W., Grob, K., *J. Chromatogr.* 1983, *254*, 265 – 269.

[19] Ewels, B. A., Sacks, R. D., *Anal. Chem.* 1985, *57*, 2774 – 2779.

[20] Hopkins, B. J., Pretorius, V., *J. Chromatogr.* 1978, *158*, 465 – 469.

[21] Klemp, M. A., Akard, M. L., Sacks, R. D., *Anal. Chem.* 1993, *65*, 2516 – 2521.

[22] Tian, W. C., Chan, H. K. L., Pang, S. W., Lu, C. J., Zellers, E. T., *IEEE International Solid-State Sensors and Actuators Conference, 8 – 12 June 2003, Boston, MA, USA*, IEEE: Piscataway, NJ, USA 2003, pp. 131 – 134, vol. 131.

[23] Tian, W. C., Pang, S. W., Lu, C. J., Zellers, E. T., *J. Microelectromech. Sys.* 2003, *12*, 264 – 272.

[24] Lu, C. J., Tian, W. C., Steinecker, W. H., Guyon, A., Agah, M., Oborny, M. C., Sacks, R. D., *et al.*, *Lab On A Chip* 2005, *5*, 1123 – 1136.

[25] Lu, C. J., Tian, W. C., Steinecker, W. H., Guyon, A., Agah, M., Oborny, M. C., Sacks, R. D. *et al.*, *Seventh International Conference on Miniaturized Chemical and Biochemical Analysis Systems – TAS, 03*, Squaw Valley, CA 2003, p. 411.

[26] Libardoni, M., Sacks, R., *Anal. Chem.* (in press).

[27] Whiting, J. J., Lu, C. J., Zellers, E. T., Sacks, R. D., *Anal. Chem.* 2001, *73*, 4668 – 4675.

[28] Wireless Integrated Micro System (WIMS) Engineering Research Center (ERC) at the University of Michigan, Ann Arbor, MI 48109.

[29] Grall, A., Leonard, C., Sacks, R., *Anal. Chem.* 2000, *72*, 591 – 598.

[30] Leonard, C., Grall, A., Sacks, R., *Anal. Chem.* 1999, *71*, 2123 – 2129.

